Progress In Electromagnetics Research, PIER 45, 201–215, 2004

WAVE PROPAGATION AND REFLECTION IN THE IONOSPHERE. AN ALTERNATIVE APPROACH FOR RAY PATH CALCULATIONS

S. A. Isaakidis and T. D. Xenos

Department of Electrical and Computer Engineering
Aristotle University of Thessaloniki
54006 Thessaloniki, Greece

Abstract—In this work, the ray trajectory for oblique incidence is determined by solving the wave equation using the Finite Element Method (FEM). In case of ionospheric reflection the Discrete Fourier Transform (DFT), applied here in the space domain, is used to discriminate the incident and reflected waves. Ray tracing equations are combined with the Poynting vector components in order to calculate the wave trajectory taking into account the Earth's curvature. The results are illustrated for different frequencies and angles of incidence using electron density profiles obtained from the Rome digisonde station, topside profiles from the IRI-95 model and atmospheric data from the MSIS-E-90 model of NSSDC as an inputs.

1. INTRODUCTION

The exact knowledge of the ionospheric or transionospheric ray path is a useful tool in many applications such as terrestrial HF radio-links, satellite communications, oblique-incidence sounding [1] and ionospheric irregularities detection [2]. There are many studies dealing with the ray path calculations. For example in [3] the Finite Differences Time Domain (FDTD) method for large distance oblique incidence ionospheric wave propagation is used. In [4] an analytical ray tracing method is presented, while in [5] ray path parameters are computed using the sech^2 model including ionospheric irregularities.

In this work, the ray trajectory for oblique incidence is determined by solving the wave equation using the Finite Element Method (FEM). Using fundamental equations from the ionospheric propagation theory, well discussed in books like [6], [7] and [8], the medium is introduced via the height profile of the refractive index, which is the main input parameter to the wave equation. In case of reflection from the ionosphere the Discrete Fourier Transform (DFT), applied here in the space domain, is used to discriminate the incident and reflected waves. The ray tracing equations are combined with the wave's propagating angle using the Poynting vector components in order to calculate the two-dimensional wave trajectory. The effect of the Earth's curvature is included in the ray path calculations while the Earth's magnetic field is not taken into account and thus the ionosphere is dealt with as an isotropic medium.

The method is illustrated using vertical electron density data obtained from the Rome (41.9°N, 12.5°E) ionosonde (November 29, 2000, 06:05–06:55 LT), combined with topside profiles, extracted using the International Reference Ionosphere, IRI-95 model (http://nssdc.gsfc.nasa.gov/space/model/models/iri.html). An interpolation method using spline functions around the F2 layer maximum electron density (NmF2) was employed to obtain a smooth transition between the two profiles. The collision effect in the lower ionospheric levels is introduced using a theoretical model proposed by [7], which is fitted with O_2, N_2 and O densities obtained from the Mass Spectrometer and Incoherent Scatter Extended Atmospheric (MSIS-E-90) model of NSSDC (http://nssdc.gsfc.nasa.gov/space/model/models/msis.html).

2. THE WAVE EQUATION

The use of the Maxwell's equations for propagation in ionosphere leads to two different sets of equations:

$$\frac{\partial E_y}{\partial z} = jkH_x, \qquad \frac{\partial H_x}{\partial z} = jkq^2(z) \cdot E_y \tag{1}$$

$$\frac{\partial E_x}{\partial z} = jk\frac{q^2(z)}{n^2(z)}H_y, \qquad \frac{\partial H_y}{\partial z} = -jkn^2(z) \cdot E_x \tag{2}$$

The two sets of Equations (1), (2) have been extensively discussed in [6]. The first one, which is used in this study, depends on E_y, H_x and H_z components and it corresponds to a horizontally polarized wave, having only the horizontal E_y component of the electric field. The second set of equations depends on E_x, E_z and H_y and corresponds to a vertical polarized wave. Elimination of H_x from the first set (1) gives:

$$\frac{d^2E_y}{dz^2} + k_0^2q^2(z)E_y = 0 \tag{3}$$

Where:

$k_0 = \omega/c$	is the wave factor
f and $\omega = 2\pi f$	are the frequency and angular frequency of the propagating wave respectively,
$q(z)$	is the vertical component of the refractive index, expressed as:

$$q^2 = \left(C^2 - X/U\right)^{1/2} = \left(\cos^2(\phi_{in}) - X/U\right)^{1/2} \tag{4}$$

where:

$$X = \omega_N^2/\omega^2 = Ne^2/\left(\varepsilon_0 m\omega^2\right), \text{ with } \omega_N^2 = e^2N/(\varepsilon_0 m) \tag{5}$$

In the above Equations (4), (5):

φ_{in}	is the incident angle of the wave,
$\omega_N = 2\pi f_N$	is the angular plasma frequency,
f_N	is the plasma frequency,
$e = 1.602 \cdot 10^{-19}$ As	is the elementary charge,
$m = 9.109 \cdot 10^{-31}$ Kg	is the electron mass,
$\varepsilon_0 = 8.854 \cdot 10^{-12}$ As/Vm	is the permittivity of vacuum,
N	is the electron density, which is a function of height and
U	is a complex quantity that introduces the collision effect defined as :

$$U = 1 - jZ = 1 - j\frac{v}{\omega} \tag{6}$$

where: v is the collision frequency.

The collision frequency model used in this study is [7]:

$$v = 3.3 \cdot 10^{-16}\sqrt{T}\,[N(O_2) + N(N_2) + 2 \cdot N(O)] \tag{7}$$

where $N(O_2)$, $N(N_2)$ and $N(O)$ are the densities in m^{-3} of O_2, N_2 and O in the atmosphere. The temperature is in $^\circ K$ and the collision frequency is given in $\sec^{-1}$.

Equation (3) is a wave equation and can be considered a special one-dimensional form of the general Helmholtz equation:

$$-\frac{d}{dz}\left(a\frac{dE}{dz}\right) + \beta E = f \tag{8}$$

with $\alpha = 1$, $f = 0$ and $\beta = -k_0^2 q^2$. The above equation does not have closed form solutions in terms of known functions, although approximate techniques have been developed such as the WKB technique. In this study a full-wave highly accurate computational treatment of Equation (3) is performed using the FEM.

3. FEM FORMULATION

For the solution of the wave Equation (3) the one-dimensional FEM was used and the problem was treated introducing a global mesh of 200000 line elements. A spline interpolation technique was used for the calculation of the refractive index at all levels, having each line element assigned to the corresponding refractive index value. The boundary conditions applied at the entrance and exit nodes have the form:

$$\left[a\frac{dE}{dz} + \gamma E\right]_{z=z_{\max}} = g \tag{9}$$

For the entrance boundary located at $z = z_{\min} = 90\,\text{Km}$ a generalized inhomogeneous Neumann boundary condition (Leontovich condition) was applied in order to permit the propagation of the up-going wave and also to absorb any possible reflections from higher ionospheric layers. The parameters for this condition are:

$$\begin{aligned} a &= 1 \\ \gamma &= ik_0 q(z_{\min}) \\ g &= 2ik_0 q(z_{\min}) \end{aligned} \tag{10}$$

For the exit boundary at $z = z_{\max} = 700\,\text{Km}$ a generalized Neumann or (first order Mur) absorbing boundary condition was applied in order to eliminate reflections from this node. The parameters for this condition are:

$$\begin{aligned} a &= 1 \\ \gamma &= ik_0 q(z_{\max}) \\ g &= 0 \end{aligned} \tag{11}$$

The solution of the problem described above, can be obtained by seeking the stationary point of an appropriate functional $F(E)$, under the given Dirichlet boundary condition. The functional can, in general, be written [9] as:

$$F(E) = \frac{1}{2}\int_{z_{\min}}^{z_{\max}} \left[a\left(\frac{dE}{dz}\right)^2 + \beta E^2 \right] dz - \int_{z_{\min}}^{z_{\max}} f_s E dz + \left[\frac{\gamma}{2}E^2 - gE\right]_{z=z_{\max}} \tag{12}$$

Where $\beta = -k_0^2 q^2$ and $f_s = 0$. By the use of linear interpolation functions we obtain an approximation of the field within each element, which, combined with the functional leads to a system of $N_{el} + 1$ equations with $N_{el} + 1$ unknowns, where the total number of elements is equal to $N_{el} = 200000$. For the solution of the system of equations the conjugate gradients squared method was used.

4. WAVE DISCRIMINATION

In the case of transionospheric propagation the solution of the wave equation returns the simple up-going wave calculated at each node of the FEM mesh. On the other hand, when the real part of the vertical component of the refractive index takes zero values, the wave is reflected from the ionosphere and the solution is the combination of the incident and the reflected wave:

$$E_{\text{total}} = E_{\text{incident}} + RE_{\text{reflected}} \tag{13}$$

where: R is the reflection coefficient.

An example of the reflection condition is illustrated in Figure 1, where the real and imaginary parts of the refractive index are shown around the reflection level. It can be seen that the real part of the refractive index reduces until it is zeroed at the height of reflection. Then, the imaginary part takes large negative values obstructing the propagation of waves above this point. The exact reflection height, H_r can be determined by the amplitude minimum of the complex refractive

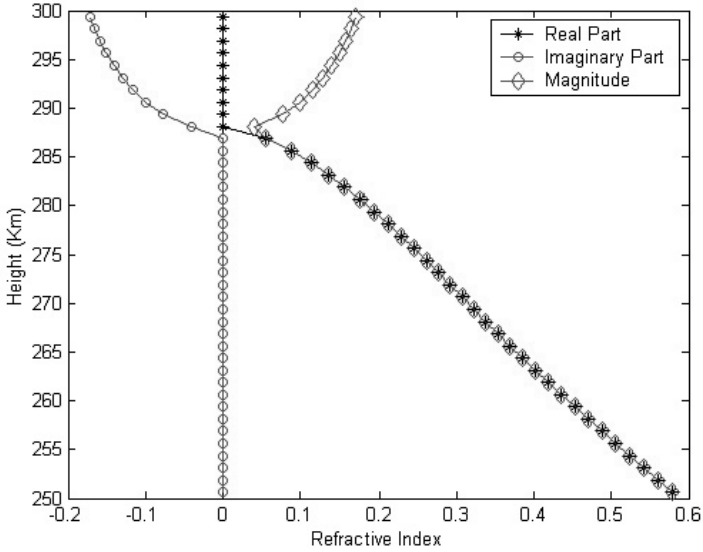

Figure 1. Refractive index around the reflection level.

index (Figure 1). The real part of the total solution for the above case, obtained by FEM, is shown in Figure 2. Applying the Discrete Fourier Transform (DFT), computed with a Fast Fourier Algorithm (FFT), to the total field, the frequency components of the incident and the reflected waves can be revealed (Figure 3). In this figure the power spectral density of the frequency components of the total field versus a normalized frequency axis are shown. The higher frequency component represents the incident wave while the lower one represents the reflected wave. The details "*a*" and "*b*" show the information included in the high power levels of these components. The DFT is given by:

$$E_F(k) = \sum_{i=1}^{M} E(i)\omega_M^{(i-1)(k-1)} \tag{14}$$

M is the number of FEM nodes that the solution is computed and
ω_M is an Mth root of unity given by :

$$\omega_M = e^{-\frac{2\pi j}{M}} \tag{15}$$

Applying independently the inverse transform to the two frequency

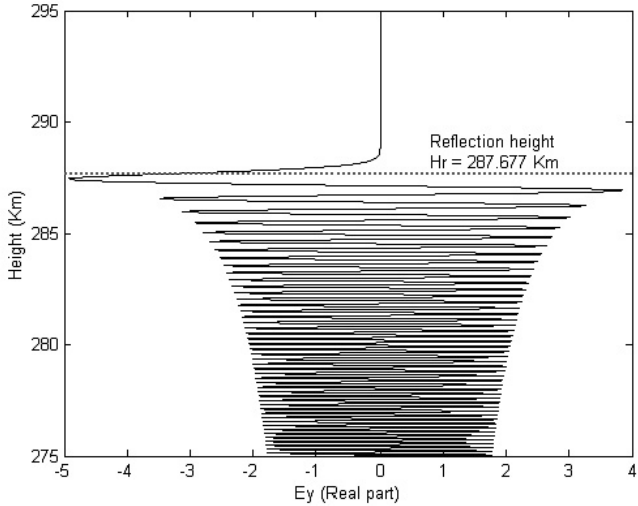

Figure 2. Real part of the total field (incident+reflected).

components the incident and reflected waves are calculated:

$$\begin{aligned} E_{\text{incident}}(i) &= \sum_{k=1}^{M} E_F^{\text{incident}}(k)\omega_M^{-(i-1)(k-1)} \\ E_{\text{reflected}}(i) &= \sum_{k=1}^{M} E_F^{\text{reflected}}(k)\omega_M^{-(i-1)(k-1)} \end{aligned} \tag{16}$$

where ω_M is given by Equation (15).

Taking into account that after the reflection point the total field is zeroed, as it can be seen from Figure 2, the transmission coefficient is $T = 0$ and thus the reflection coefficient can be taken as $R = 1$, which means that the total field is simply the sum of the incident and reflected waves.

The wave discrimination described above can be further clarified with the following analytical example. Assuming an up-going incident wave with the general form of $E_{\text{inc}} = E_0 e^{-jk_0qz}$, the corresponding reflected down-going wave will be $E_{\text{inc}} = E_0 e^{jk_0qz}$. The Fourier transform of these waves results in two waves with shifted frequency components, which are included in the reconstructed total wave:

$$\left.\begin{aligned} E_F^{\text{inc}}(\omega) &= 2\pi E_0 \delta(\omega + k_0 q) \\ E_F^{\text{ref}}(\omega) &= 2\pi E_0 \delta(\omega - k_0 q) \end{aligned}\right\}$$
$$\Rightarrow E_F^{tot}(\omega) = 2\pi E_0 \left[\delta(\omega + k_0 q) + \delta(\omega - k_0 q)\right] \tag{17}$$

where E_0 is the amplitude of the wave and δ is the Dirac delta function.

5. THE WAVE TRAJECTORY

Since the E_y component of the wave is computed using the FEM, the H_x and H_z components can be obtained by post processing, using [6]:

$$\sin(\phi_{in})E_y = H_z \tag{18}$$

$$\frac{\partial E_y}{\partial z} = jk_0 H_x \tag{19}$$

Since the effect of the Earth's magnetic field is neglected, the medium is dealt with as isotropic and thus the energy flow, determined by the Poynting vector, is parallel to the direction of propagation. Applying Equations (18) and (19) all the wave components are known and in this case the x and z components of the Poynting vector can be calculated as:

$$P_x = \frac{1}{2}\mathrm{Re}\left(E_y H_z^*\right) \tag{20}$$

$$P_z = -\frac{1}{2}\mathrm{Re}\left(E_y H_x^*\right) \tag{21}$$

The angle of the wave with respect to the vertical z-axis in $+\infty$ is:

$$\phi = \tan^{-1}\left(\frac{P_x}{P_z}\right) \tag{22}$$

As the wave starts from the initial height H_0 and propagates to higher ionospheric layers, it's direction lies on the positive x and z-axis and therefore P_x, P_z are positive. In case of reflection, P_x is still positive but P_z takes negative values. This means that the wave travels downwards in the same x direction. In this case the angle of the wave with respect to the vertical z-axis in $-\infty$ is given by:

$$\phi = \tan^{-1}\left(\frac{P_x}{|P_z|}\right) \tag{23}$$

Assuming that the ionosphere is divided into a number of very thin layers equal to the number of the mesh elements used for the solution and that inside each layer the medium properties are constant, the angle φ describes the different angles of the wave for the whole propagation path.

The geometry of propagation is shown in Figure 4. Using this geometry as a reference and following the initial steps of ray tracing analysis [10] the wave's trajectory can be calculated.

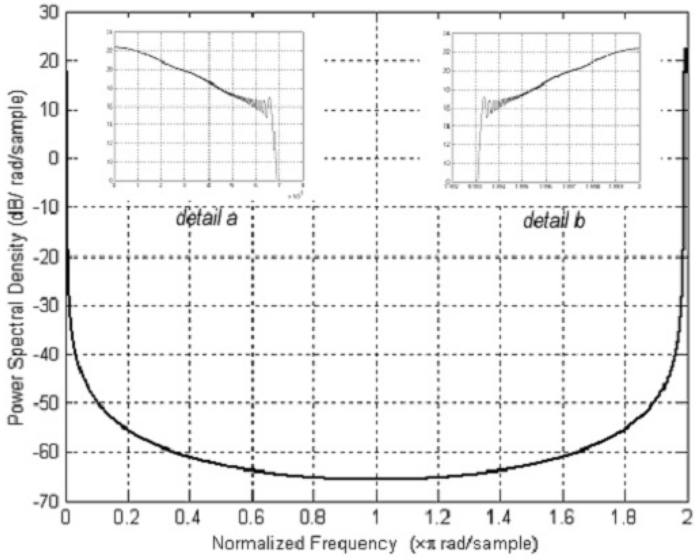

Figure 3. Frequency components of the total wave.

A Cartesian coordinate system (x, z) is assumed with its axis center $O(0, 0)$ being center of the Earth. The wave path starts at layer n_1 from the point $A(x_A, z_A) \equiv A(0, R_1)$ with $R_1 = R_0 + H_0$, where $R_0 = 6378165\,\text{m}$ is the Earth's radius and $H_0 = 90\,\text{Km}$ is the initial height. The wave propagates inside layer n_1 having an initial angle of $\varphi_{in} = \varphi_1$ and reaches the point $B(x_B, z_B)$. The coordinates of this point are given by:

$$\begin{aligned} x_B &= R_2 \cdot \sin(d\theta_1) \\ z_B &= R_2 \cdot \cos(d\theta_1) \end{aligned} \tag{24}$$

where:

$$R_2 = R_0 + H_0 + dz_1 \tag{25}$$

The quantity dz_1 expresses the depth of the current layer where the refractive index is assumed constant and thus the propagation angle of the wave remains unchanged. dz_1 is a priori known since it corresponds to the distance between the two first nodes of the FEM mesh.

From the triangle OAB:

$$(180 - \phi_1) + \psi_1 + d\theta_1 = 180, \quad \text{or} \quad d\theta_1 = \phi_1 - \psi_1 \tag{26}$$

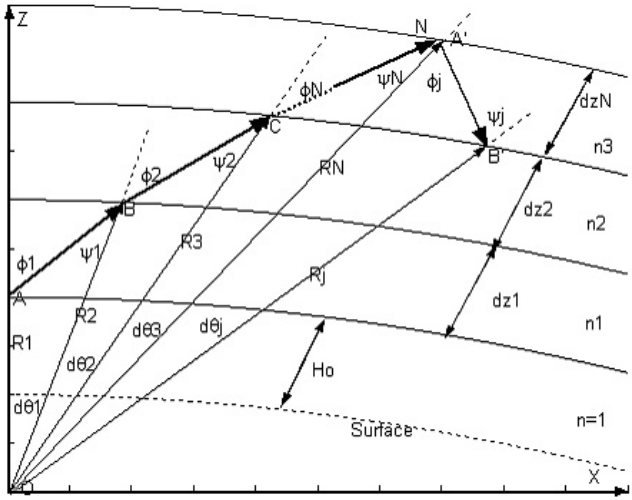

Figure 4. Propagation geometry.

$$\frac{R_1}{\sin(\psi_1)} = \frac{R_2}{\sin(\phi_1)}, \quad \text{or} \quad R_2 \cdot \sin(\psi_1) = R_1 \cdot \sin(\phi_1) \tag{27}$$

From Equation (27) the angle ψ_1 is calculated:

$$\psi_1 = \arcsin\left(\frac{R_1 \cdot \sin(\phi_1)}{R_2}\right) \tag{28}$$

The angle ψ_1 is already known, since it is the initial angle of incidence and thus combining Equations (26) and (28) the angle shift, $d\theta_1$ of the wave inside the layer n_1 can be computed:

$$d\theta_1 = \phi_1 - \arcsin\left(\frac{R_1 \cdot \sin(\phi_1)}{R_2}\right) \tag{29}$$

Inserting equations (29) and (25) to equation (24) the coordinates of the point B are determined.

Continuing in the same manner for the next point $C(x_C, z_C)$:

$$\begin{aligned} x_C &= R_3 \cdot \sin(d\theta_1 + d\theta_2) \\ z_C &= R_3 \cdot \cos(d\theta_1 + d\theta_2) \end{aligned} \tag{30}$$

with:

$$R_3 = R + H_0 + dz_1 + dz_2 \tag{31}$$

The angle ψ_2 of the triangle OBC is calculated similarly to Equation (28) as:

$$\psi_2 = \arcsin\left(\frac{R_2 \cdot \sin(\phi_2)}{R_3}\right) \tag{32}$$

and thus for $d\theta_2$:

$$d\theta_2 = \phi_2 - \arcsin\left(\frac{R_2 \cdot \sin(\phi_2)}{R_3}\right) \tag{33}$$

The angle φ_2 is calculated using Equation (22). From Equations (30), (31), (32) and (33) the coordinates of point C are computed. In general, for any given point $N(x_N, y_N)$, it can be showed that:

$$\begin{aligned} x_N &= R_N \cdot \sin\left(\sum_{i=1}^{N} d\theta_i\right) \\ z_N &= R_N \cdot \cos\left(\sum_{i=1}^{N} d\theta_i\right) \end{aligned} \tag{34}$$

$$R_N = R + H_0 + \sum_{i=1}^{N} dz_i \tag{35}$$

$$d\theta_i = \phi_i - \arcsin\left(\frac{R_i \cdot \sin(\phi_i)}{R_{i+1}}\right) \tag{36}$$

In case of reflection the angle φ_j (Figure 4) is calculated using Equation (23). The same set of equations can also be used for the reflected wave, inserting the angle φ_j with negative sign. From the triangle $OA'B'$:

$$\phi_j + (180 - \psi_j) + d\theta_j = 180, \quad \text{or} \quad d\theta_j = \psi_j - \phi_j \tag{37}$$

Equation (37) is an inverse form of Equation (26) and thus by setting the negative angle φ_j these two equations take the same form since the minus sign is also transferred to ψ_j through Equation (28).

6. RESULTS AND DISCUSSION

In order to illustrate the method, vertical electron density data obtained from the Rome (41.9°N, 12.5°E) digisonde, combined with topside profiles, extracted using the IRI-95 model, were used. The chosen date is the 29$^{\text{th}}$ November 2000 and the time period 06:05–06:55 LT. Some of the main corresponding geomagnetic and solar indices

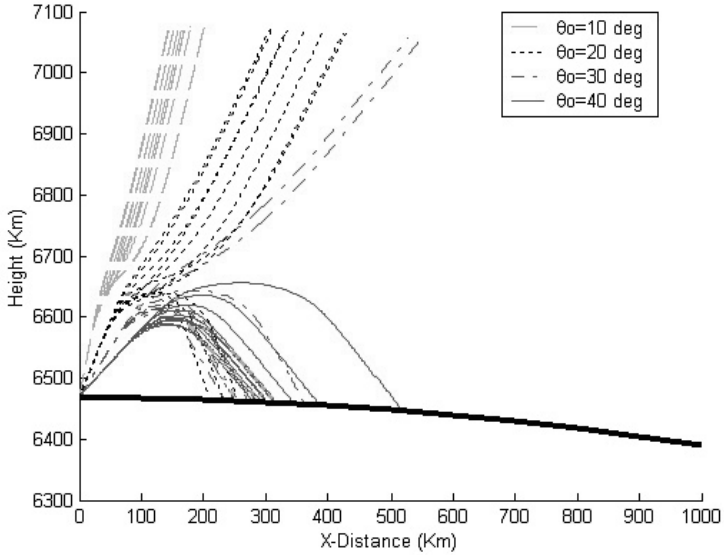

Figure 5. Ray paths starting from various angles of incidence.

obtained from the World Data Center for Solar-Terrestrial Physics (Chilton, WDC-C1, http://wdcc1.bnsc.rl.ac.uk/wdcc1/data.html), are: Ap=111nT, IG=137.6, IG_{12} = 137.8, SSN(daily)=123, R_{z12} = 112.4. An interpolation method using spline functions around the NmF2 was employed to obtain a smooth transition between the two profiles. The collision model of Equation (7) is fitted with O_2, N_2 and O densities obtained from the MSIS-E-90 atmospheric model of NSSDC.

An informative example of the results obtained following the above procedures is illustrated in Figure 5. In this example the ray paths for various angles of incidence are shown. The sets of rays were calculated for the angles of 10°, 20°, 30° and 40° with respect to the vertical and each ray corresponds to a different ionospheric profile, while the time interval between them is 5 minutes. The solid thick bottom line represents the equivalent Earth's surface at the altitude of 90 Km. It can be seen that as the elevation angle is decreasing, more rays are reflected from the ionosphere, while the reflection takes place at different heights due to the different levels of the refractive index magnitude minimization.

In Figure 6 the ray paths for two different operating frequencies (f_1 = 7.5 MHz, f_2 = 8.5 MHz) are shown. The angle of incidence for both ray sets is 20°, while the ionospheric conditions are the same as

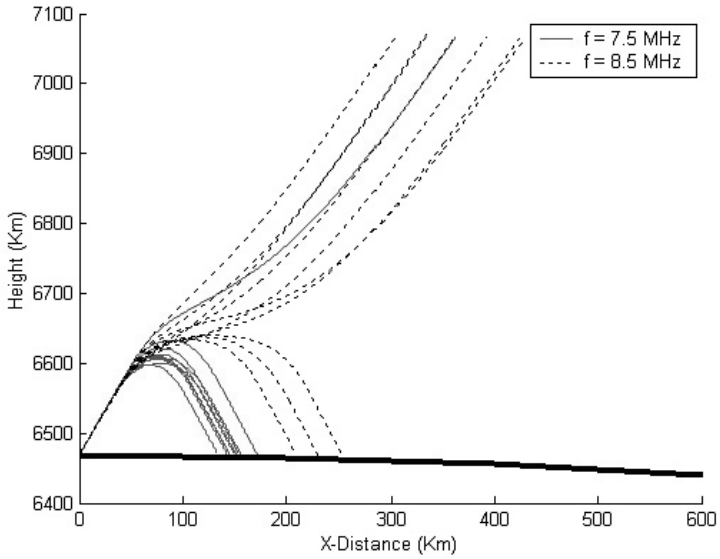

Figure 6. Ray paths for different frequencies (Angle of incidence = 20°).

those used in the example of Figure 5. It is obvious that when f_1 is used almost all rays are reflected from the ionosphere, since for the most profiles f_1 is below the Maximum Usable Frequency (MUF). Using the higher frequency, more rays propagate through the ionosphere and the reflected waves travel greater distance since the reflection takes place at higher altitudes.

The method described in this work can be readily applied to transionospheric propagation too, since the solution of the wave equation directly returns the main wave components and thus main parameters such as amplitude, phase advance and angle can be easily calculated. On the other hand the use of the DFT and IDFT for the wave discrimination makes the ray paths calculation in the case of ionospheric reflection possible. Since the medium properties are numerically applied for each node of the FEM mesh, there is no need for analytical electron density profiles, while ionospheric media including inhomogeneities or irregularities can be modeled very efficiently. Also, the method can be used for different elevation angles and higher frequencies taking into account that the computational cost is higher since a more dense mesh is required.

ACKNOWLEDGMENT

Special thanks are due to Dr. Vincenzo Romano from Instituto Nationale di Geofisica e Vulcanologia of Rome, for supporting this work by providing the Rome vertical ionosonde data.

REFERENCES

1. Krasheninnikov, I. V., J. C. Jodogne, and L. F. Alberca, "Compatible analyses of vertical and oblique sounding data," *Annali di Geofisica,* Vol. XXXIX, No. 4, 763–768, 1996.
2. Danilkin, N. P. and C. L. Tolsky, "Transionospheric radio sounding and NH-profile determination," *XXIVth General Assembly of the URSI*, Kyoto, Japan, 1993.
3. Xenos, T. D. and T. V. Yioultsis, "An FDTD method with oblique incidence for ionospheric wave propagation problems — Application to an HF one-hop radiolink study," *IEEE Trans. on Magnetics,* Vol. 38, No. 2, 677–680, March 2002.
4. Mlynarczyk, J., J. Caratori, and S. Nowak, "Analytical calculation of the radio wave trajectory in the ionosphere," *XXIVth IMAPS Poland Conference,* Poland, 2000.
5. Lundborg, B., R. Lindström, and A. Västberg, "The sech^2-model in new applications," *Sixth International Conference on HF Radio Systems and Techniques,* IEE Conf., IRF-U nr 413, 74–80, 1994.
6. Budden, K. G., *The Propagation of Radio Waves,* Cambridge University Press, Cambridge, 1985.
7. Yeh, K. C. and C. H. Liu, *Theory of Ionospheric Waves,* Academic Press, London, 1972.
8. Davies, K., *Ionospheric Radio,* Peter Peregrinus Ltd, 1990.
9. Jin, J., *The Finite Element Method in Electromagnetics,* John Wiley & Sons Inc., 1993.
10. Lear, M. W., "Refraction corrections equations and tables," NASA Mission Planning and Analysis Division, Lyndon B. Johnson Space Center, 1979.

Stergios A. Isaakidis received a Diploma in Electrical Engineering from the Engineering Department of the Hellenic Air Force Academy and he is a Ph.D. Candidate in Aristotle University of Thessaloniki. He is Electronic Intelligence officer and Communications and Electronic Warfare engineer in the Hellenic Air Force.

Thomas D. Xenos received a Diploma in Electrical Engineering from the University of Patras and a Ph.D. in Radio Wave Propagation from the Aristotle University of Thessaloniki. He is Associate Professor of Electrical Engineering in the Aristotle University of Thessaloniki.